1 Introduction

1.1 Nanostructures

Nanostructures are being investigated intensively because of their distinctive properties that make them potential candidates for advanced technological applications. As a result, many methods have been developed for the fabrication of nanoscale objects.[3]

Nanotechnology, which is the study of manipulating matter on an atomic or molecular scale, has witnessed considerable progress with the synthesis and characterization of nanoparticles over the last three decades. Initially, a significant breakthrough was achieved by the synthesis of (spherical) nanoparticles with a controlled composition. With the knowledge that the physical and chemical properties of nanostructures are highly dependent on their size, shape, and dimensionality, many researchers have investigated methods for producing novel nanostructures. Presently, a large variety of nonspherical nanostructures can be synthesized.[4–9] At some point, new terms and definitions will be required to accommodate new nanomaterials.

The objective of existing standardized nanotechnology definitions and taxonomies is to clarify the terminology. Nanomaterials – the all-encompassing term for materials having one or more nanoscale external dimensions or a nanoscale internal or surface structure – include two main types, according to the International Organization for Standardization (ISO): nano-objects and nanostructured materials (Figure 1.1).[10] The latter exhibit nanoscale internal or surface structures, whereas nano-objects are defined as particles with one, two, or three nanoscale external dimensions.[11]

Among these nano-objects, one-dimensional (1-D) nanostructures (or nanofibers) such as wires, tubes, and rods represent a very interesting class of nanomaterials. 1-D nanostructures having two similar nanoscale external dimensions and a significantly larger third dimension represent suitable systems for investigating mechanical and transport properties with respect to size reduction.[12] In particular, nanowires are attractive not only for nanoscience studies but also as interconnects and functional elements of novel devices for applications such as electronic circuits, optoelectronics, energy harvesting, and (electro-)catalysis. Nanowires exhibit many properties that are similar and others that are considerably different from those of their macroscopic counterparts, including large surface-to-volume ratios and increased scattering of electrons. However, nanowires often facilitate independent control of several properties, which is not possible on the macroscale.[13]

Driven by the expected technological impact, studies on nanowires have gained substantial importance. Consequently, several methods have been developed for the synthesis of nanowires with well-defined dimensions, morphology, crystal structure, and composition.[12,14] A large variety of synthetic approaches are adopted to achieve 1-D growth, such as anisotropic crystal growth, vapor phase methods, and self-assembly of 0-D nanoparticles; however, some of the most general techniques are based on the use of templates.[12] Frequently used hard-template materials for nanowire fabrication are anodic aluminum oxide (AAO) and ion-track etched membranes, which can be filled, e. g., by electrochemical deposition.

1.2 Complex nanowire systems

Nanoparticles often do not exist as individual nano-objects, but in large quantities, forming assemblies that can be much more extensive than their nanoscale components. On the basis of the interactions between nanoparticles, terms were introduced to specify nanostructured materials (Figure 1.1).[10]

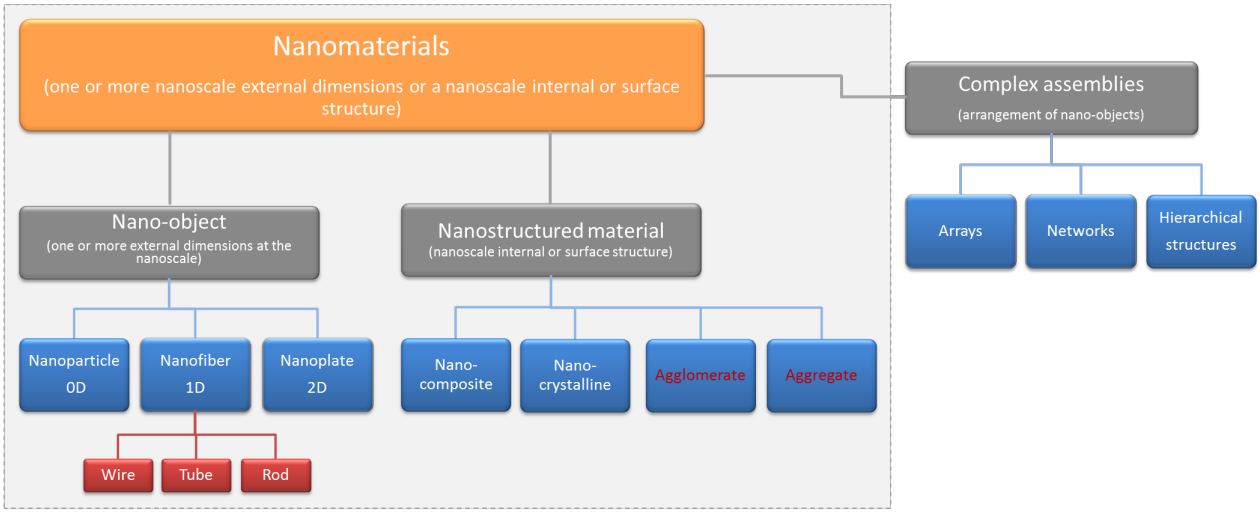

Figure 1.1: Scheme showing terms and definitions of nanomaterials. The terminology is partly adopted from reports published by the International Organization of Standardization (ISO definitions are highlighted in grey). [10,11]

An agglomerate is a collection of loosely bound particles or aggregates, whereas particles that are strongly bonded or fused form an aggregate. For an agglomerate, the resulting external surface area (SA) is comparable to the sum of the SAs of the individual nanoscale components, while for an aggregate, the SA is significantly smaller than the sum of the SAs of the components. [11]

In the field of nanoscience, complex assemblies of nanostructures are being investigated intensively. In comparison to individual nanoparticles, complex assemblies often exhibit new functionalities or a substantial improvement in their properties. [15] Because many characteristics depend on the orientation, complexity, integration level, and interconnectivity, organization of nanoscale building blocks into superstructures is crucial for various applications.

Nanowires are potential building blocks for the synthesis of complex assemblies. The diversity of the ultimate functionalities of several complex nanowire systems has been demonstrated. A common approach to organizing nanowires into superstructures is the fabrication of nanowire arrays. In addition, superstructures that differ from arrays, which represent only one very fixed kind of interconnectivity, have been reported, including networks and hierarchical structures (Figure 1.1).

However, the controlled synthesis of nanowire assemblies is currently at a nascent stage. Efficient generalized methods are required for the organization of nanowires into various superstructures with controlled interconnectivity. To understand and predict the collective behavior of integrated nanowires, it is necessary to create increasingly complex building block assemblies and to elucidate their fundamental properties. Thus, potential applications can be defined for different kinds of assemblies. [16]

1.3 Objective of the thesis

Compared to the numerous studies on nanowire synthesis, research on 3-D nanowire assemblies is rather limited. This field is crucial for the development of nanowire-based devices that require a high integration level of nanowires. General assembly methods are very important, especially if they allow the extension of existing approaches and readily make nanowires available for macroscopic applications.

A conventional approach for nanowire growth is the ion-track template electrodeposition method, which has been frequently adopted to grow nanowires with excellent control over wire morphology and crystallinity. [14,17] Although this synthesis route has been known for decades, its development has mainly focused on the growth process for producing novel or improved 1-D nanostructures using template

materials with parallel aligned nanochannels; very few reports deal with nanowire assemblies deviating from arrays.[18]

In this thesis, the method is extended to organize nanowires into complex assemblies, starting from the conventional fabrication technique. Focus should be put on the design of 3-D architectures consisting of numerous nanowires by a simple deposition process. In addition, the possibility of growing various complex arrangements of nanowires, resulting in integrated nanowire superstructures of macroscopic dimensions, should be investigated.

Central to the concept is the idea that the advanced design of 3-D nanowire assemblies with improved properties requires both controlled nanostructuring and architectural design. A general method that meets these requirements would overcome the limitations of current template materials by allowing independent control of (i) the characteristics of individual nanowires (including dimensions and composition) and (ii) the arrangement of nanowires into various assemblies. On the basis of further development, if possible, different types of assemblies can be synthesized with integrated nanoscale building blocks, whose structures have the same qualities as those of nanowires created in traditional templates. It is important to investigate such assemblies in order to understand their special properties. Hence, potential applications may be identified. The collective behavior of integrated nanostructures is expected to strongly depend on arrangement, integration level, and degree of interconnectivity. Figure 1.2 shows the general pathway for this thesis, from controlled synthesis of nanowires to their organization into complex assemblies, and the understanding of their properties provides new opportunities. We must focus on these fundamental aspects.

An additional challenge for this study is to investigate whether the ion-track template electrodeposition method can be enhanced with respect to control over the structure, morphology, composition, and size of individual nanowires.

Platinum is selected as the nanowire material for this study because electrodeposition into nanochannels of track etched polycarbonate has been reported previously.[19] As a noble metal, Pt is suitable for demonstrating novel nanowire structures and nanowire assemblies effectively. To verify the general applicability of the developed method, other materials may also be used.

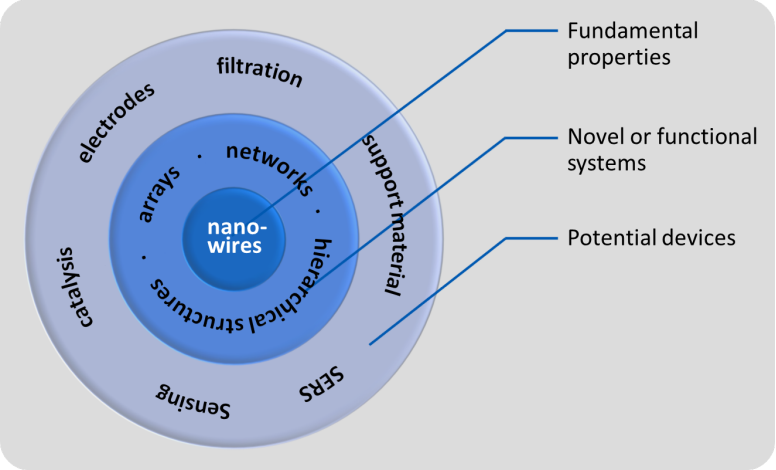

Figure 1.2: Scheme highlighting the pathway from nanowires to 3-D nanowire building block assemblies. The fabrication of different nanowire assemblies and the investigation of their functional properties is a key issue that must be addressed in order to define potential device functions.

The main text of this thesis is organized into eight chapters: The next chapter (chapter 2) describes the ion-track template method and basic concepts related to the growth of nanowires via electrodeposition into nanochannels. Chapter 3 evaluates strategies that have been reported for creating various complex nanowire assemblies, as well as their properties and potential applications. Chapter 4 describes the

experimental details for all investigations performed within this thesis. Chapters 5 and 6 highlight the experimentally obtained results for the fabrication and characterization of nanowires and nanowire building block assemblies, respectively.

The final chapters (chapters 7 and 8) conclude the thesis with a discussion of the main results, followed by plans for future work. Additional information on nanowires and nanowire assemblies, which is not presented in the main text, can be found in the appendix.

2 Nanowires by template electrodeposition - basic concepts

Template electrodeposition constitutes one of the most general methods to achieve 1-D growth.[12] In this straight forward approach, the nanostructures are grown electrochemically inside a hard-template material adopting its shape. Usually, the host material exists in form of a porous membrane. Frequently used are AAO and ion-track etched polymer templates. The preparation of nanomaterials using templates has been reviewed among others by Hulteen and Martin, and, more recently, by Kline et al.[14,20]
It is difficult to scale up the fabrication process due to the limited volume of the thin membranes, but excellent control over nanowire dimensions and composition can be reached. Furthermore, the benefit of the method lies within the possibility to produce arrays of parallel aligned nanowires, which often allow the easy examination of numerous nanowires at once.
Template based electrodeposition has been known for decades. It was first reported by Possin, who synthesized nanowires in tracks obtained by etching fission tracks in mica crystals, in the late 1960s.[21]
Today, a large variety of template materials is available and nanowires of different materials were produced by electrodeposition including metals, semiconductors and conductive polymers. The electrodeposition parameters can have a strong influence on the composition and crystal structure.
In this chapter, the ion track template electrodeposition method, whose fundamental ideas are of vital importance for this work, is illuminated. Basic concepts that have been demonstrated by previous reports in this field are discussed extending from ion matter interactions, appearing at the very beginning of template fabrication, to electrocrystallization in fluidic nanochannels, taking place during formation of the nanowires. Finally, the producible nanostructures with their peculiar properties are addressed.

2.1 The ion-track template electrodeposition method

The ion track template electrodeposition method is based on templates fabricated by the irradiation of membranes with swift heavy ions in combination with chemical track-etching technique.[22] The pore diameter is controlled by the etching time. Nanowires of the desired material are generated by electrochemical reduction of ions from an electrolyte solution adopting the shape of the cylindrical nanochannels. Prior to electrodeposition, a conductive metal layer is sputter deposited on one side of the membrane to serve as cathode for the nanowire growth. A schematic of the fabrication process is depicted in Figure 2.1.

Figure 2.1: Scheme of the ion-track template electrodeposition method

Commonly used as template material are polymers such as polycarbonate (PC) or polyethylene terephthalate (PET). For instance, the use of PC templates was reported by Penner and Martin.[23,24]
Compared to AAO, which is also widely employed and commercially available, the pores of track-etched polymer membranes are randomly scattered across the surface. The pore density can be adjusted covering a wide range between 1 - 10^{10} pores per square centimeter for nanowire production. It is worth

mentioning that porous polymer membranes are chemically inert with respect to most electrolytes, allowing, in contrast to AAO, the deposition of nanowires from a broad range of electrodeposition baths including strong acidic and alkaline solutions. Moreover, the polymer foils can easily be handled, since they are very flexible.

2.1.1 Template fabrication

Although polymer templates can be obtained commercially, it is advantageous to produce the templates by means of a heavy-ion accelerator – in spite of the considerable effort. This approach is of course necessary to control all parameters allowing the fabrication of templates designed for certain experiments. It may be considered essential in order to fully understand all aspects and advance the ion-track template electrodeposition method.
Basic concepts of ion irradiation and chemical etching are explained in the following.

Ion irradiation

Heavy ions with kinetic energies of approximately 10 MeV/u can be employed for template fabrication. When ions that are highly positively charged penetrate a solid-state material, energy is transfered due to various processes as the ions slow down until they come to rest inside the material or escape from it. Knowledge about the basic principles of interactions, which are involved in energy transfer, is crucial to understand track formation.

Energy loss

Decisive for heavy ions of several MeV/u are interactions with electrons and nuclei of the target. Thus, the total energy loss is the result of two main contributions, electronic energy loss $\left(\frac{dE}{dx}\right)_e$ and nuclear energy loss $\left(\frac{dE}{dx}\right)_n$:

$$\left(\frac{dE}{dx}\right) = \left(\frac{dE}{dx}\right)_e + \left(\frac{dE}{dx}\right)_n \tag{2.1}$$

The interaction cross-section is correlated to the ion velocity. At low ion velocities (energy $\leq$0.01 MeV/u), elastic collisions with the target atoms are dominant. At higher velocities (>0.1 MeV/u), energy is transfered predominantly by interactions between the heavy ion and the electrons of the target atoms resulting in electronic excitation and ionization processes. The electronic energy loss is described by the Bethe-Bloch equation:

$$\left(\frac{dE}{dx}\right)_e = \frac{4\pi \cdot e^4 \cdot Z_{eff}^2 \cdot Z_t \cdot N}{m_e \cdot v^2} \left[\ln\left(\frac{2m_e \cdot c^2 \cdot \beta^2}{I}\right) - \beta^2 - \delta - U\right] \tag{2.2}$$

with
- e = elementary charge
- Z_{eff} = effective charge of the ion (in units of electron's charge)
- Z_t = atomic number of target element
- N = density of the target atoms
- m_e = electron mass
- v = velocity of the ion
- I = ionisation energy
- β = speed v of the ion relative to that of light
- δ = term correcting for relativistic effects
- U = low velocity correction for non-participation of inner electron shells

Depending on the velocity, an ion of atomic number Z, moving through a solid, captures or looses electrons. The changed charge state is taken into account by introducing an effective charge Z_{eff}, which is given by an empirical formula:

$$Z_{eff} = Z\left[1 - \exp\left(-\frac{130\beta}{Z^{2/3}}\right)\right] \tag{2.3}$$

The energy loss depends on Z_{eff}, which in turn is a result of interactions of the projectile with the electrons around the atoms in the target. The types of collisions, in which the ion is involved, are a strong function of its velocity.
At high velocities, the ion is being stripped of all its orbital electrons, and $Z_{eff} = Z$. Interactions of the highly charged ion, moving through the solid, with electrons of target atoms are a consequence of electrical forces. Hence, electrons are ejected from the target atoms or are excited to higher energy levels. The ejected electrons (δ electrons) can provoke further excitation and ionization spreading radially from the core of the ion track. Because heavy ions with a higher atomic number Z acquire a higher effective charge Z_{eff}, their electronic energy loss is higher.
While the heavy ion passes through the solid material, it is slowed down and can gradually reacquire its electrons, as the kinetic energy decreases. Finally, elastic collisions with target atoms become the dominant process (nuclear energy loss). For example, the calculated total energy loss and the contributions from nuclear and electronic energy loss are shown in Figure 2.2a for an Au ion with an initial kinetic energy of 12 MeV/u. The inset depicts the region of lower kinetic energy where the nuclear energy loss becomes larger than the electronic one (0.01 MeV/u) and finally dominates the total energy loss as the ion energy is further decreased.

Ion range

The total range R (average projected range) of an ion in the target material is determined by the initial kinetic energy of the ion E_0 and its specific energy loss along the trajectory:

$$R = \int_0^{E_0} \left(\frac{dE}{dx}\right)^{-1} dE \tag{2.4}$$

The ion range can be calculated by means of equation 2.4. Different codes are available such as the SRIM2008 code that was used here.[25,26] For instance, Au ions of a kinetic energy of 11.1 MeV/u have a calculated range of approximately 170 µm in polycarbonate as indicated in Figure 2.2b which depicts the ion range plotted versus the ion energy.

Ion track formation in polymers

In polymers, the interactions with energetic heavy ions result in a permanent modification of the material along the ion path. Primary and secondary excitation and ionization processes lead to the formation of a cylindrical damage zone, the so-called latent track. In this damage zone, various processes occur including chemical bond breaking and formation of unsaturated bonds and other functional groups. In Figure 2.3a, track formation involving chain scission is schematically illustrated. Altered physical and chemical behavior of the tracks allows the transformation into nanochannels by selectively removing material.

Important for the fabrication of polymer templates is the applied fluence Φ, which is defined as the total number of ions that intersect a unit area during the irradiation experiment. The fluence has units of cm^{-2} and is the ion flux integrated over time.

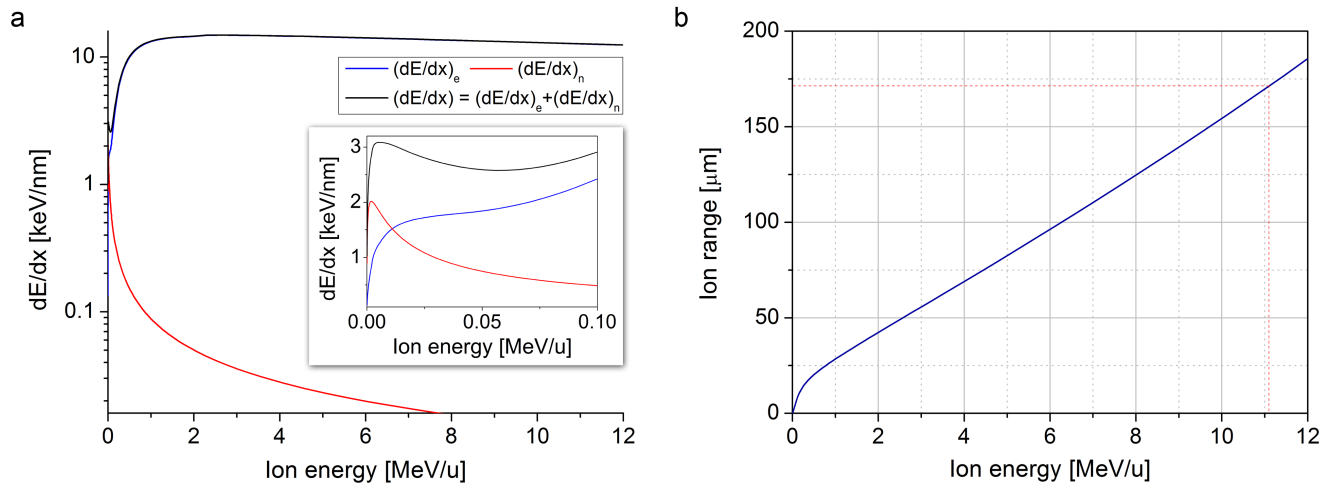

Figure 2.2: Energy loss and ion range calculated for Au ions in polycarbonate using the SRIM2008 code. (a) Total energy loss and its two contributions, electronic and nuclear energy loss, as function of the ion energy. The inset depicts the region of low ion energy. (b) Ion range plotted versus the ion energy. As indicated by red lines, Au ions of a kinetic energy of 11.1 MeV/u have a range of approximately 170 μm.

Chemical etching

Nanochannels are created inside irradiated polymer membranes by preferentially removing the material of the latent tracks using chemical etching. The etching process may be regarded as a competition of two etching rates: chemical etching along the latent track at a linear etching rate v_T and a general dissolution on the surface of the etched polymer at a slower rate v_G (Figure 2.3b).
The pore shape depends on the ratio of the etching rates. If the track etching rate is much higher than the general etching rate ($v_T \gg v_G$), a nanochannel with almost cylindrical geometry will be obtained. Figure 2.3b illustrates how the etching process creates a cone with the original ion track in its center. The cone angle γ, given by equation 2.5, becomes larger the smaller the etching rate ratio v_G/v_T is.

$$\gamma = \arcsin\left(\frac{v_G}{v_T}\right) \tag{2.5}$$

The ratio of the etching rates can be influenced by using different etching solutions and additives and etching from both sides. Consequently different channel geometries, including conical, bi-conical, and funnel shaped nanochannels, are obtained. With varying v_T along the track the channel geometry will become convex or concave. Tracks tilted at an angle α to the surface lead to elliptic intersections of the track with the surface after etching.
For the fabrication of nanowires, cylindrical nanochannels are predominantly used. In the case of ion-track etched polycarbonate membranes, the aspect ratio of channel diameter to length is limited to a maximum of roughly 1:1000 for a cylindrical channel geometry due to the etching process.[27]

2.1.2 Nanowire growth by electrodeposition

The synthesis of nanowires by electrodeposition is based on the reduction of ions from an electrolyte solution inside nanochannels of the template material. The reduction of metal ions from an aqueous solution can be described as follows:

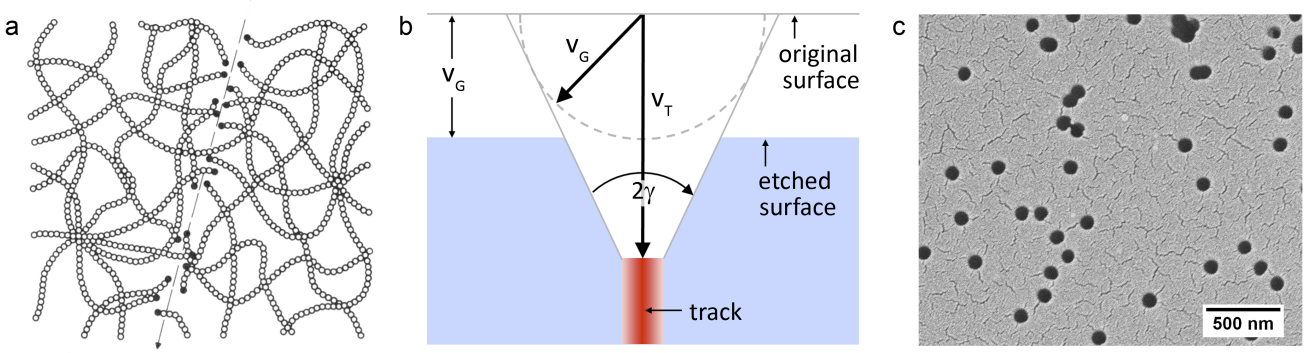

Figure 2.3: Ion tracks in polymers: (a) Track formation involving chain scission and the formation of new functional groups.[22] (b) Schematic of the track etching process with general etching rate v_G and track etching rate v_T. (c) SEM image of an ion-track etched polycarbonate foil showing randomly distributed nanochannels (ϕ=10^9 ions/cm^2).

$$M_{aq}^{z+} + z \cdot e \leftrightharpoons M_{solid} \tag{2.6}$$

where M^{z+} is an ion of the charge state $z+$.

During electrodeposition electrons are supplied by an external current source. Two electrodes (cathode and anode) are immersed in an electrolyte solution containing metal ions. The metal ions are reduced at the interface of the cathode and deposit in the metallic state. Therefore, the process described by means of equation 2.6 is a reaction that takes place at the phase boundary between metal electrode and solution involving charged particles. Both metal ions and electrons can pass through the phase boundary. The direction of the reaction depends on the electrochemical potential of the metal species in the electrode $\overline{\mu}_e$ and in the solution $\overline{\mu}_s$.

If an electrode is in contact with an electrolyte solution (half-cell), a potential difference is generated due to charge carriers passing through the phase boundary. The electrode is characterized by the electrode potential E. The electrode potential of an electrode is the voltage measured against a reference electrode without a flow of current. Electrode potentials allow the calculation of the cell potential of an electrochemical cell consisting of two half-cells. In addition, the potential required for electrolysis can be estimated.

The **Nernst equation** correlates electrode potential E with activities of the ions (Equation 2.7). It is of major significance for electrochemistry.

$$E = E^0 + \frac{RT}{zF} \ln \frac{a_{Ox}}{a_{Red}} \tag{2.7}$$

with E^0 denoting the standard potential, R the universal gas constant, T the absolute temperature, z the number moles of electrons being transferred in the reaction, F the Faraday constant, and a_{Ox} and a_{Red} the activity of the relevant oxidized and reduced metal species, respectively. The Nernst equation is only valid for electrodes in the electrochemical equilibrium state, when there is no current flow.

The potential of an electrode in an electrochemical cell can be shifted from the equilibrium potential by applying an external potential. Consequently, the system reacts to the new potential by changing the concentrations of the electrochemically active species at the electrode surface, trying to reach equilibrium conditions again. Chemical reactions take place and an electrical current flows. The deviation of the

applied potential from the electrode equilibrium potential is called overpotential η. The electrical current density depends on the overpotential. The correlation is given by the **Butler-Volmer equation** taking into account anodic and cathodic reactions:

$$j = j_0 \left[e^{-\frac{\alpha F \eta}{RT}} - e^{\frac{(1-\alpha) F \eta}{RT}} \right] \tag{2.8}$$

with j_0 = exchange current density
η = overpotential
α = symmetry factor (dimensionless)

The exchange current density j_0 indicates kinetic limitations of the electrical charge transfer at the electrode. The so-called symmetry factor α describes the ratios of the slopes of anodic and cathodic reaction and ranges from 0 to 1.

In electrolysis, the reaction rate of a system can be easily controlled by selecting the overpotential as means of adjusting the driving force for the reaction. With increasing cathodic overpotential the concentration of the electrochemical active species, reacting at the cathode, is increasingly reduced in the immediate vicinity of the electrode until every incoming ion is directly reduced. The reaction becomes limited by mass transport processes arising from the depletion of cations in the diffusion layer. The current stays constant even if the overpotential is further increased. This current, limited by diffusion, is denoted diffusion threshold current I_d. In the case of convection, the diffusion layer is of constant thickness δ (stationary case). Mass transport can be described by Fick's first law of diffusion, and the limiting current I_d (at an electrode with the area A) only depends on the bulk electrolyte concentration c_0:

$$I_d = nFAD \cdot \frac{c_0}{\delta} \tag{2.9}$$

In stagnant solution, the diffusion layer is not constant in time as described by Fick's second law and the resulting current becomes time-dependent. As the diffusion layer grows with $\sqrt{t}$, the current decreases with $1/\sqrt{t}$. This current decay is given by the **Cottrell equation**:

$$I = \frac{nFA\sqrt{D}}{\sqrt{\pi t}} \cdot c_0 \tag{2.10}$$

Equation 2.10 is strictly valid only in the case of planar diffusion that is observed for electrodes with a large surface area of macroscopic dimensions.

Research within the field of electrodeposited nanowires by template based methods requires – in addition to knowledge of macroscopic concepts – the consideration of special effects involved in mass transport and phase formation in confined space on the nanoscale. Important aspects of transport processes in fluidic nanochannels and low-dimensional metal phase formation will be discussed in separate sections (2.2, 2.3). At first, an overview of the preparation of various structured nanowires by different electrodeposition techniques is given in the following subsection (2.1.3).

2.1.3 Structured nanowires

To provide nanowires with novel catalytic, electrical, optical, and magnetic properties, methods have been developed to prepare multilayered or barcode nanowires consisting of different materials.[28] As consequence of the segmented structure based on different compositions, these nanowires can show multiple functionalities and enhanced properties in comparison to their single-component counterparts. The template-based method also proved to be an effective approach for obtaining length and sequence controlled multicomponent layered structures using sequential electrochemical deposition of several segments (of metals, polymers, composites) as shown in Figure 2.4.[28,29]
Growth of segments of different composition is achieved by time-consuming synthesis involving multiple plating steps from different plating solutions or by pulsed electrodeposition from a single-plating solution containing ions of different elements.[30] Using a single bath, various multilayered nanowires including Ag/Co, Au/Co, Bi/Sb, Bi/BiSb, Co/Cu, Co/Pt, Fe/Au, and Ni/Cu have been produced by template electrodeposition.[31–38] The composition of segments is controlled by the pulse potential, while the length L is adjusted by the pulse duration. In addition to pulsed electrodeposition methods, segment formation can also by reached by CV deposition techniques.[39]

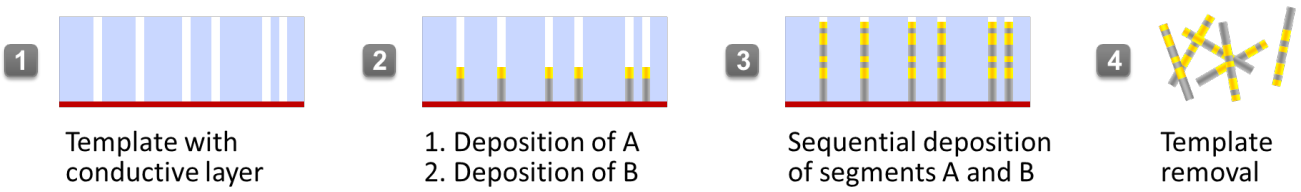

Figure 2.4: Template electrodeposition of multilayered nanowires based on length and sequence controlled segments of different compositions A (gray) and B (yellow).

In Figure 2.5 TEM images of multilayered Fe/Au and Co/Pt nanowires are given.[36,37] Due to different densities the metal segments can be clearly identified using a transmission detector.
While extensive research work has been dedicated to segmented multicomponent nanowires, whose readily distinguishable structure elements are made of different compositions, only scarce knowledge is available about segmented 1-D nanostructures consisting of constant composition or only one chemical element.[40]
For example, diameter-modulated 1-D nanostructures were obtained by Huang et al. using electrodeposition on a glass substrate without a template. Periodically structured straight cobalt filaments formed by the spontaneous oscillation of the electric voltage.[41] Matthias et al. described modulated Au microwires prepared by electroless deposition into membranes with controlled variation of the channel diameter with the channel depth.[42] In the case of templates with continuously cylindrical nanochannels, Wang et al. created shape-tailored porous gold nanowires with segments of different diameters and lengths by applying postdeposition processing to cylindrical multisegment gold-silver alloy nanowires with segments of different compositions.[40] Very recently, Shpaisman et al. reported the deposition of CdSe nanowires with constant diameter and uniform chemical composition, but exhibiting modulated "density" along the wire axis.[39] However, segmented single-element nanowires can not be directly synthesized in cylindrical nanochannels by the template electrodeposition methods reported so far.
Studies on nanowires have shown that their properties (e.g., thermal conductivity, electrical conductivity, catalytic and optical properties) depend not only on size, and crystallinity, but also on the nanowire morphology.[43–45] In particular, surface roughness has been demonstrated to play a crucial role in the decrease of thermal conductivity in Si nanowires, and interesting plasmonic effects have been predicted also for nanowires showing constrictions along their length.[46,47]
Successful manipulation and additional control of the morphology of nanowires, electrodeposited inside

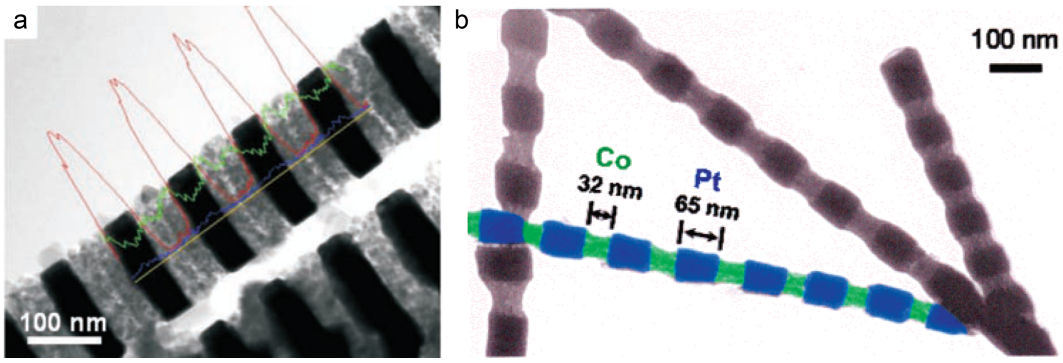

Figure 2.5: TEM images of multilayered nanowires produced by pulse electrodeposition from a single bath using AAO templates: (a) Fe/Au nanowires. Reprinted with permission. Copyright 2005 American Chemical Society.[37] (b) Co/Pt nanowires. Copyright Wiley-VCH Verlag GmbH & Co. KGaA. Reproduced with permission.[36]

templates, would open up new opportunities to tune the surface characteristics of nanowires for specific thermal, catalytic, and optical applications.

2.2 Transport processes

The study of transport processes of fluid in and around structures with features that measure less than 100 nm in at least one dimension is termed nanofluidics. In this confined structures, the occurrence of phenomena that are impossible at larger length scales is observed. Nanofluidics constitutes a relative young research field, which has achieved considerable growth in the last years. It has been reviewed by various reports.[48–50]

Here we focus on the processes and mechanisms relevant for nanowire growth in ion-track etched polymer membranes. Emphasis is put on surface-charge-governed transport including electrokinetic effects. However, the main transport process during nanowire growth is diffusion that will be addressed starting with a description of the diffusion modes towards nanowires, growing inside nanochannels, at different growth stages. In contrast to macroscopic electrodes, diffusional mass transport can be extremely efficient to nanoelectrodes.
It has to be considered that the production of nanowires involves both special transport processes in nanofluidics and those at nanoelectrodes.

2.2.1 Diffusion to nanoelectrodes

Ultrasmall electrodes with dimensions on the micrometer scale or smaller have typical attributes that are different from macroscopic electrodes. Depending on their actual size, they are known as micro-, ultramicro- or nanoelectrodes.[51]
Nanowires are a special kind of nanoelectrodes, which show the typical properties of microelectrodes to a greater extent, including small charging currents, short response times, and enhanced mass transport. The latter is of particular importance for electrodeposition, since reduction at the cathode (and hence, the growth rate) is in this process often controlled by the flux of ions to the electrode surface. The diffusion is not constant in time. It starts with the build up of a concentration gradient, when applying, e.g., a potential that is sufficient to reduce the active ion species instantaneously at the electrode-electrolyte interface so that the reaction becomes diffusion controlled after a short time.

Mass transport to single nanoelectrodes

The time evolution of the current, after applying the potential step in a simple chronoamperometry experiment, can be obtained by solving Fick's second law, using the appropriate boundary conditions as described elsewhere.[52,53] For small electrodes, additional diffusion processes besides planar diffusion have to be taken into account.
With decreasing radius of a small disk electrode mass transport proceeds not only perpendicular to the electrode surface, but also parallel to the electrode. This transition between planar and hemispherical diffusion is a consequence of the electrode size. The same behavior is observed for progressing time. The diffusion layer grows with the measurement period and thus covers an increased solid angle. Consequently, the flux of ions per time and area unit is significantly higher than in the case of purely planar diffusion. In addition, the transport process becomes stationary after a certain time and the diffusion layer is of constant thickness. The current can be described as function of time by a **modified Cottrell equation**.[53] For a disk electrode with radius r_0 it is:

$$I(t) = \frac{nFA\sqrt{D}}{\sqrt{\pi t}} \cdot c_0 \left(1 + b\sqrt{\frac{Dt}{r_0}}\right) \tag{2.11}$$

The coefficient b describes the transition between a planar and a hemispherical diffusion field ($\sqrt{\pi} \leq b \leq 4/\sqrt{\pi}$). It approaches $4/\sqrt{\pi}$ as mass transport becomes dominated by hemispherical diffusion. Equation 2.11 demonstrates a time-independent and a time-dependent term contributing to the current. Expressions for the short-time and long-time limits can be specified.

Short-time limit

For very short times the diffusion layer is considerably smaller than the electrode radius. Diffusion proceeds linearly to the electrode surface. The first term of equation 2.11 is significantly larger than the second one at these short times, and the current is Cotrellian. It decays according to equation 2.10 with $1/\sqrt{t}$.

Long-time limit

After a certain time, a hemispherical (three-dimensional) diffusion field is established. A constant limiting current is reached as the time-independent second term of equation 2.11 becomes dominant. This steady-state value of the current is given by:

$$I_d = \frac{nFAD}{r_0} \cdot c_0 \tag{2.12}$$

The steady-state current depends on the electrode geometry. Equations for recessed disk, inlaid disk, and hemisphere electrodes are given together with schemes of the diffusion modes in Figure 2.6. All three described electrode types are observed during electrodeposition using the ion-track template method, since they represent nanowires at different states of growth. Thus, transitions in diffusion modes are indicated by changes in the measured current.[54,55]

Mass transport to nanoelectrode arrays

In contrast to single nanoelectrodes, the diffusion fields of growing nanowires can not be regarded as independent from each other for template electrodeposition of nanowire arrays. Overlap of hemispherical diffusion zones around individual nanoelectrodes has to be taken into account. Interactions between

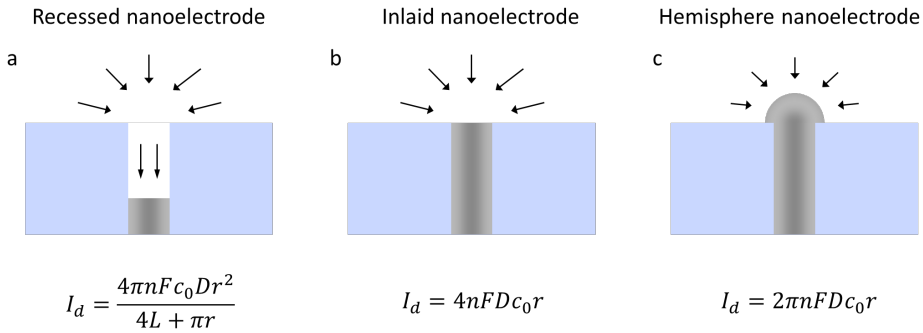

Figure 2.6: Scheme of diffusion modes to single nanowire electrodes deposited in nanochannels at different growth states. Adapted by permission of The Royal Society of Chemistry.[51]

hemispherical diffusion fields occur as soon as the distance between electrodes becomes comparable with the diffusion layer thickness.[56]

At short times, planar diffusion to individual nanowire electrodes is observed and the current is described by equation 2.10 with respect to the electrochemically active surface area (ECSA), which is the sum of the area of all electrodes from the array. Depending on the average interelectrode distance, after an intermediate stage of partially coupled spherical diffusion zones, the diffusion zones may completely overlap, and the current becomes Cotrellian to the total surface area as mass transport is linear to the whole plane. The current in these limiting regimes is not affected by the distribution of the nanoelectrodes across the surface, whereas a considerable deviation arises at the transition between spherical to planar diffusion for different array geometries. Mass transport to several types of microelectrode arrays including square lattice, hexagonal lattice, and random array has been precisely considered, e.g., by Scharifker.[56]

The nanoelectrode density is of particular importance for the diffusion processes and the limiting current density. In the case of arrays with low nanochannel density, the hemispherical diffusion to individual nanoelectrodes can independently proceed for rather long times or even throughout the entire deposition process (Figure 2.7a), while dense nanowire arrays show linear diffusion shortly after the growth was initiated (Figure 2.7b).

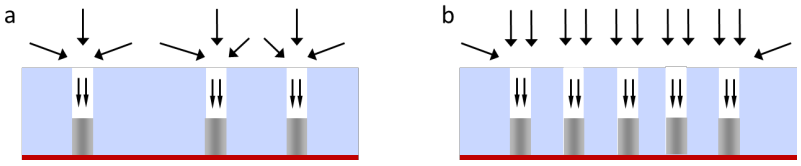

Figure 2.7: Scheme of diffusion modes to nanowire electrode arrays growing in templates of different nanochannel densities: (a) low density array with individual diffusion regimes; (b) high density array with overlapping diffusion regimes.

2.2.2 Transport phenomena in nanofluidics

Fluidic nanochannels exhibit, due to their small dimensions, a whole range of phenomena that are based on various forces including surface energy, electrical double layer, size, and entropy related effects.[48] Here, only fundamental concepts of electrostatics in liquids and electrokinetic effects, which are important for nanowire electrodeposition in polymer membranes, are briefly introduced.

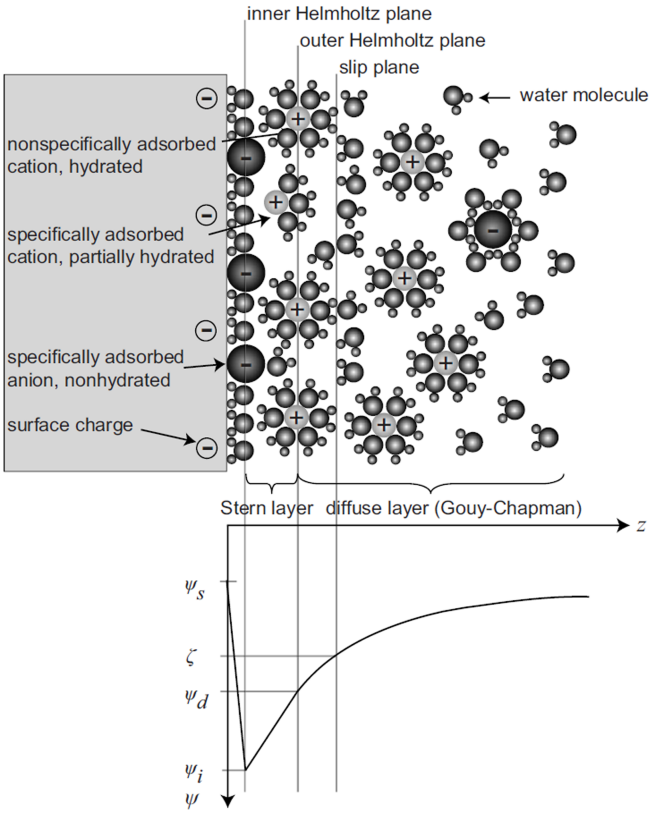

Figure 2.8: Scheme of the solid-liquid interface and the potential distribution according to the Gouy-Chapman-Stern model. The solid surface acquired a negative potential Ψ_s. The EDL can be separated in the solution in three layers. Inner and outer Helmholtz plane consist of nonhydrated coions and counterions, and only hydrated counterions, respectively. Beyond the slip plane is the diffuse layer. In this third layer the concentration of mobile coions and counterions is determined by a competition of electrostatics and diffusion processes. The ζ-potential at the slip plane can be experimentally determined and is usually equal to the potential of the outer Helmholtz plane (Ψ_d). Adapted with permission from Schoch et al.[62] Copyright 2005, American Institute of Physics.

Electrostatics in liquids

Fixed surface charges at solid interfaces in contact with a solution can be acquired by various mechanisms including specific ion adsorption, direct ionization of surface groups, differential solution of surface ions, and substitution of surface ions.[57,58] In particular, polymer surfaces are known to contain surface groups such as carboxyl, hydroxyl, amino, and sulfonic acid groups that can be directly ionized. The degree of dissociation of these groups depends on the pH value.
The net surface charge density can be given in units of charge per area (e.g., C/cm^2).[59]

Electrical double layer

Considering a solid-liquid interface, a fixed surface charge at the solid interface results in the creation of a region of opposite charge in the solution. This separation of charge is called electrical double layer (EDL).[60] Different models to describe the structure of the EDL have been developed. The Gouy-Chapman-Stern model, which is schematically shown in Figure 2.8 with the corresponding potential distribution, separates the EDL in three layers.[49] In the first layer, the so-called inner Helmholtz plane, not hydrated coions and counterions are specifically adsorbed on the surface. The inner Helmholtz plane has the potential Ψ_i. A layer of bound hydrated, and partially hydrated counterions constitutes the outer Helmholtz plane, which is the second layer with the potential Ψ_d. Inner and outer Helmholtz planes are components of the Stern layer. The third layer is a diffuse layer consisting of mobile ions. It begins with the so-called slip plane, which is characterized by the ζ-potential. The ζ-potential can by determined by electrokinetic measurements and allows an estimation of Ψ_d.
The potential distribution in the EDL is described by the Poisson-Boltzmann equation. Different solutions for this partial differential equation have been described including the Debye-Hückel approximation and the Gouy-Chapman equation. A detailed analysis is outside the scope of this text, but further information can be found in various reports.[49,61]

From a simplistic point of view, it can be assumed that the potential decays exponentially across the diffuse layer with the distance z from the interface. The potential is given (Debye-Hückel approximation) by:[57]

$$\Psi = \Psi_d exp(-\kappa z) \tag{2.13}$$

where κ is the Debye-Hückel parameter. Its reciprocal value is the Debye length λ_D that describes the thickness of the EDL.

$$\lambda_D = \kappa^{-1} = \left(\frac{\epsilon_0 \epsilon_r k_B T}{2 N_A e^2 I_s} \right)^{1/2} \tag{2.14}$$

with ϵ_0 = permittivity of free space
ϵ_r = relative permittivity
k_B = Boltzmann constant
N_A = Avogadro constant
I_s = ionic strength $I_s = \frac{1}{2} \sum_i c_i z_i^2$, where c_i is the concentration and z_i the valency of ion i.

The thickness of the EDL depends on the ionic strength, showing a decrease in length with increasing I_s, which in turn is linked to the ion concentrations.
In the case of fluidic nanochannels, the EDL thickness can be the same order as the channel diameter. Consequently, a large part of the channel is subjected to interactions with the EDL resulting in shaping of local electrolyte distributions and velocity profiles. As the Debye length becomes larger than the nanochannel radius, double layers from opposite walls overlap and the potential can be different from zero everywhere inside the channel.[63]

Electrokinetic effects in nanochannels

Due to charges at interfaces parts of the EDL experience movement under an applied electrical field. These phenomena are studied in the field of electrokinetics and include electroosmosis and electrophoresis. It has to be considered that electrokinetic effects can have a strong influence on the local ion concentration inside nanochannels. Therefore, it is important to note the fundamental concepts, which also may be relevant for nanowire growth.

Electroosmosis

In presence of an electrical field, movement of the liquid relative to the stationary charged interface occurs. A net excess of positively charged ions in the diffuse layer of the EDL results in a movement to the cathode. Since the ions are solvated, also molecules from the liquid are drawn along resulting in a flow termed electroosmotic flow. In the case of nanochannels with overlapping EDLs, the profile of the flow becomes parabolic in shape, whereas a plug flow is observed for channels with diameters that are significantly larger than the EDL.[49]

Electrophoresis

Electrophoresis describes the movement of charged particles in an electrical field relative to the liquid, which is regarded as stationary. Electrophoresis is the converse of electroosmosis.[49]

During nanowire growth, of course no fluid flow can occur because the nanochannels are closed at one side by the growing nanowire. Nevertheless, mobile ions may be influenced in the stationary liquid by an electrical field.

2.3 Electrocrystallization

To study and understand the structure and properties of nanowires produced by template electrodeposition it is necessary to have some knowledge about electrocrystallization. This phase formation process involves fundamental subjects including nucleation and crystal growth. Electrocrystallization processes have been frequently studied and are often used for nanostructure synthesis. In particular, the method is widely used because it is easily possible to adjust the driving force by controlling the electrode potential.[64] Special aspects that are important for the fabrication of nanowires are briefly presented in this section.

2.3.1 Nucleation

In the case of electrodeposition, nucleus formation and crystal growth are achieved by increasing the electrochemical potential of the ions in solution $\overline{\mu}_s$ until it becomes larger than that of the ions in the solid phase $\overline{\mu}_e$. Consequently, electrochemical supersaturation, which can be defined by the difference $\Delta\overline{\mu} = \overline{\mu}_s - \overline{\mu}_e > 0$, is reached. Usually, supersaturation is induced by changing the cathodic overpotential η resulting in a first order phase transition ($\Delta\overline{\mu} = ze\eta$).[64]
On a foreign substrate, phase formation has to start with nucleation as first step in the deposition process. In order to form a new nucleus, the so-called nucleation work, a thermodynamic barrier, has to be provided. The free energy of formation of a nucleus of N atoms, $\Delta G(N)$, is given by equation 2.15.[64]

$$\Delta G(N) = -N\Delta\overline{\mu} + \Phi(N) \tag{2.15}$$

The second term $\Phi(N)$ takes into account the increase of the surface energy due to the creation of the surface of a new nucleus.[65] With increasing N, the nucleus work $\Delta G(N)$ increases until a maximum is reached and then decreases. The cluster size at the maximum is the critical nucleus size N_c. Clusters, which are larger than the critical size, can grow spontaneously while smaller nuclei tend to dissolve.
The nucleation rate *J(t)* allows a kinetic description of the nucleation process on an electrode surface. Nucleation can proceed instantaneously or progressively. Exact expressions for *J(t)* are presented elsewhere.[64,65] The nucleation rate can be influenced by the electrodeposition conditions and has a strong influence on the structure of the deposit, including crystallite size and distribution, and thus its properties.

2.3.2 Growth models

In the initial stage of growth, a growing nucleus can be regarded as independent. As the diffusion zones around individual nuclei increase in thickness with time, eventually overlap of diffusion fields has to be considered (as described in 2.2.1). This aspect will be of particular importance, if current-time relationships during growth of nuclei are considered.[65] In addition to existing clusters, whose diffusional fields increasingly overlap with time, contributions to the overall current from newly formed nuclei must not be neglected.

In principle, a coherent deposit is formed by two mechanisms that are 2-D layer growth and 3-D crystallite growth.

Layer growth

A schematic illustration of layer growth is presented in Figure 2.9a-b. This growth process is dominated by lateral spreading of layers across the surface. Depending on the electrodeposition conditions (e.g.,

overpotential), new layers start to form only after the layer, which had formed immediately before, was completed.

3-D crystallite growth

A continuous deposit can also be created by the nucleation-coalescence growth mode. In this mechanism, the first step is the independent formation of isolated nuclei and their growth to 3-D crystallites. As the crystallites partially start to coalesce, they become interconnected to a network structure. Finally, a coherent deposit is established.[65]

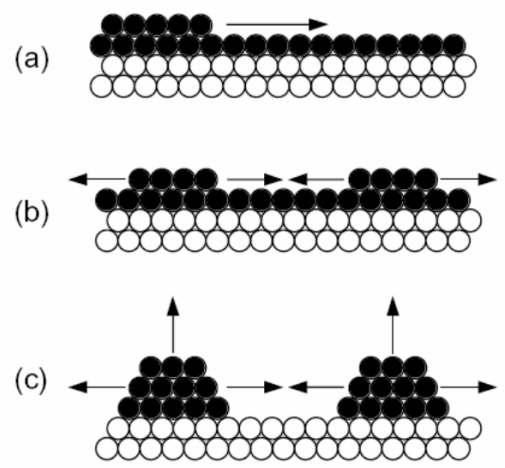

Figure 2.9: Scheme illustration basic growth mechanisms for the formation of a coherent deposit. (a-b) Layer growth mechanism. (c) Nucleation-coalescence mechanism. Copyright 2006 John Wiley & Sons, Inc. Reproduced with permission.[65]

The basic mechanisms mentioned above have been also frequently reported for electrodeposited nanowires by the template-assisted method.[34,66] It was shown that single crystalline nanowires grow according to a layer-by-layer growth mode, whereas polycrystalline wires follow a 3-D nucleation-coalescence mechanism. For instance, Dou et al. demonstrated that Bi/BiSb superlattice nanowires follow a 2D plane growth mode under certain conditions.[34] Tian et al. reported that face formation according to 2D layer-by-layer mechanismen is relatively easy to achieve for low melting point metals including Pb, Sn, Bi, Ag, Au, and Cu during template electrodeposition, while high melting point metals such as Co, Ni, and Rh tend to follow a 3-D growth mode because of higher binding energies, resulting in the preferential aggregation of atoms into small 3-D clusters.[66] It should be noted that transitions between different growth modes are known.

2.3.3 Texture formation

Textures often develop during the deposition. They are linked to the growth process and can depend on the structure of the substrate.[65]
Single-crystal substrates may exert a strong epitaxial influence on the phase formation process. Depending on the growth conditions, epitaxial crystallites will be formed, which may lead to a continuous epitaxial layer. It has to be considered that not only epitaxial nucleation and growth, but also independent nucleation and nonepitaxial growth can occur. These two competitive processes, and hence the degree of crystallite orientation, strongly depend on the deposition conditions and the electrolyte solution.
On polycrystalline substrates with random orientation of the crystallites, a texture can arise during the

deposition process. A preferred orientation of the crystallites requires an electrodeposit of a certain thickness, since texture development is based on competitive formation processes between crystallites of various orientations. These crystallites, exhibiting a preferred orientations, can come into existence either by preferential nucleation or by a competitive growth, which is based on the fact that different crystal faces show different growth rates.
In the case of a typical 3-D nucleation-coalescence mechanism, a deposit with random oriented crystallites is formed at the initial stage of phase formation. Subsequent to the stage of coalescence, a preferred orientation can develop. Amorphous substrates have no epitaxial influence on the structure of the deposit; the texture is merely governed by the growth process.
The determination of transitions in texture formation by XRD is not straightforward, since different layers of a sample contribute to the measurement. A possibility to reveal texture gradients consists in preparing electrodeposits of different thicknesses, applying the same conditions and subsequent investigation of the texture with respect to the sample thickness.
Texture formation can be influenced by the applied deposition techniques and parameters. Modern electronics that allow an exact potential to be applied as nearly any function of time have enhanced this possibility.[67]

2.3.4 Electrocrystallisation in nanochannels

Inside nanochannels, electrocrystallization is subjected to confined spaces resulting in a localized nucleation and growth process. In addition to the general principles for electrocrystallization mentioned above, special effects arising from nanochannel template structures must not be neglected.

The first step of phase formation is already important because at this stage is defined whether mononuclear or multinuclear growth modes can occur. The generation of a single nucleus inside a nanochannel, as schematically presented in Figure 2.10, can be used to grow a single crystalline nanowire, while a large number of crystallites inevitably result in a polycrystalline wire structure. However, competitive growth processes may result in a preferred crystallite orientation and the development of a columnar structure subsequent to the coalscence stage.
Depending on the growth conditions, crystallites may become comparable in size to the channel diameter.

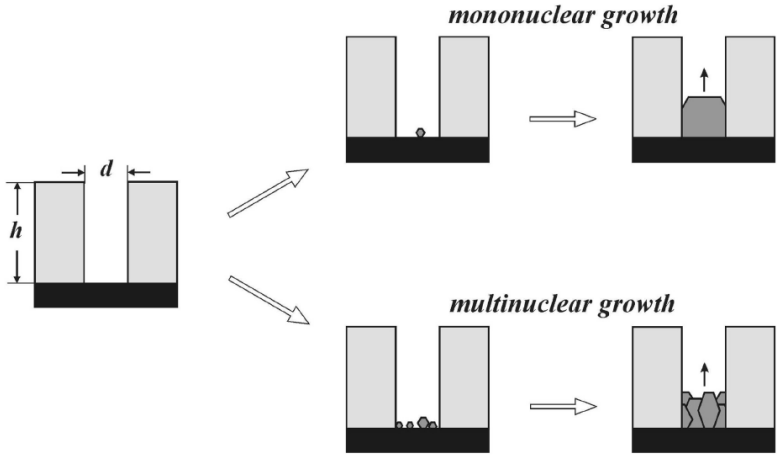

Figure 2.10: Scheme of mono- and multinuclear growth modes inside channels of a template material. Copyright 2007 Wiley-VCH Verlag GmbH & Co. KGaA. Republished with permission.[64]

2.4 Special properties of nanowires

Nanowires exhibit (as 1-D nanostructures) new physical and chemical phenomena. These peculiar and fascinating properties, which can be fundamentally different from those of their bulk counterparts, are a consequence of the reduced dimensionality and shape anisotropy. As the nanoscale building blocks promised to enable new kinds of devices and applications, they have become subject of intensive research.[12,14,68] Today, many studies are available about the properties of nanowires and how they can be tuned by controlled nanostructuring.

In this section, the impact of the reduced dimensionality on the nanostructure's characteristics is briefly addressed. For example, the transport properties based on electron interactions are explained for one-dimensional structures. Furthermore, the high surface-to-volume ratio and the consequences of the surface energy on the morphological stability are described. Focus is put only on the most important properties of nanowires that are relevant within the scope of the thesis.

2.4.1 Surface-to-volume ratio

Characteristic for nanowires is not only their small size, but also a large surface-to-volume ratio. Simple geometrical considerations lead to the fact that the specific surface area increases as the size of an object is decreased.[3] In Figure 2.11, the calculated surface area with respect to the mass of a Pt nanowire is plotted versus the wire radius assuming a cylindrical geometry and a wire length of L=30 µm. With decreasing radius the surface area increases dramatically. While wires with a radius of 50 nm have a theoretical surface area of 1.9 m^2/g Pt, the value is 18.7 m^2/g Pt for nanowires with r=5 nm.

Compared to bulk materials, nanostructures possess a large fraction of surface atoms. As a consequence, the chemical and physical properties are significantly influenced by the surface and interactions taking place at the phase boundary. Low coordinated surface atoms increasingly govern the nanowire's characteristics with decreasing diameter. This is the reason for lowering of the melting point and for an increased catalytic performance of nanostructures in comparison to their bulk counterparts.[69–71]

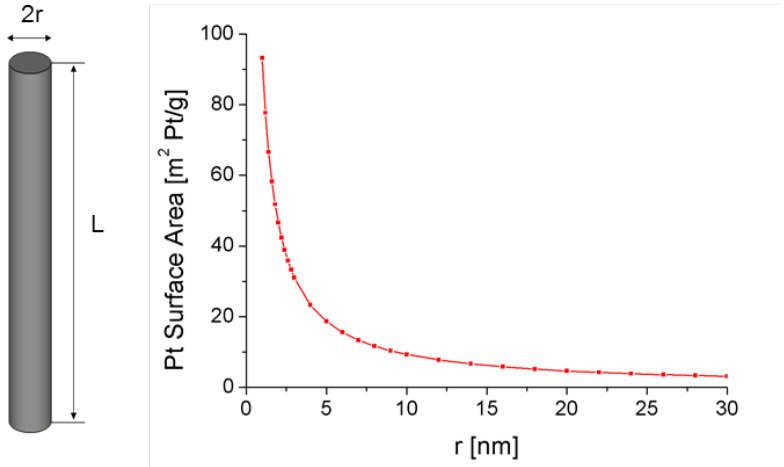

Figure 2.11: Theoretical surface area (SA) with respect to the mass versus the radius r of a Pt nanowire demonstrating a dramatic increase of SA with decreasing r. The surface area was calculated assuming a cylindrical geometry and a wire length L of 30 μm.

2.4.2 Thermal stability

The thermal stability of nanowires is crucial for their integration as functional elements in advanced technological applications. It is well-known that the melting point of bulk material is reduced when it exists as a nanostructure. This was observed for various nanoscale objects, e.g., Au nanoparticles.[3] It was also reported for nanowires that their thermal properties strongly depend on their diameter. Driven by Rayleigh instability, thin nanowires can undergo morphological transformations already at slightly elevated temperatures.

The concept of Rayleigh instability

The concept of Rayleigh instability can be traced back to studies on the instability of liquid cylinders reported by Plateau as a series of parts in the Transactions of the Brussels Academy in the 1840s. Various translations of this original work were published including a comprehensive series appearing in annual reports of the Smithsonian Institution (starting with the first part in 1863).[72] Due to minimization of the surface area and thus the total surface energy, a liquid cylinder breaks up into spherical drops under volume conservation. Plateau demonstrated that the cylinder is unstable against sinusoidal perturbations with a wavelength λ greater than the circumference $2\pi R_0$ (R_0 is the radius of the initially cylindrical liquid). Later, Lord Rayleigh continued with perturbation analysis of liquid jets and elucidated regular spacing between formed droplets and their size distribution.[73] Nichols and Mullins adopted Rayleigh's analysis to explain the instability of solid rods, which results in comparable morphological changes as observed for liquid cylinders.[74]

Rayleigh instability of metal nanowires

The analysis of Nichols and Mullins, which accounts for mass transport processes including surface and volume diffusion, has been frequently considered to describe the fragmentation of 1-D nanostructures.[75–80] Therefore, a short summary of their main conclusions is given in the following. A cylinder of infinite length (no end effect) with isotropic surface energy is analyzed with respect to variations of the radius r by surface undulation of the form

$$r = R_0 + a \sin \frac{2\pi}{\lambda} x \tag{2.16}$$

where a denotes the amplitude and λ the wavelength of the perturbation; x is the coordinate along the wire axis. A schematic illustration of a nanowire that undergoes tranformation into a chain of spheres is presented in Figure 2.12. The cylinder will become unstable against perturbations, if λ is larger than a minimum wavelength $\lambda_{min} = 2\pi R_0$. At a certain wavelength λ_{max} the perturbation growth with a maximum rate. λ_{max} is a function of the mass transport process and was specified to be 8.89 R_0, 9.02 R_0, and 12.96 R_0 for surface, internal volume, and external diffusion, respectively. It can be assumed that the distance between adjacent spheres is controlled by λ_{max}. Provided that the volume remains constant, the diameter of the spheres d_s can by calculated by $d_s = \sqrt[3]{6\lambda_{max}R_0^2}$.
Perturbations, which are not symmetric with regard to the axis, are found to be stable.

The idea developed by Nichols and Mullins has some limitations and can not explain all experimentally obtained findings in a satisfactory manner. For instance, nanowires with a single-crystalline structure do not possess isotropic surface energies resulting in higher resistance against Rayleigh instability as demonstrated by Karim et al. for Au nanowires.[81] Real nanowires are not infinite long and show end effects. Depending on their length wires can also be directly transformed into just one sphere.

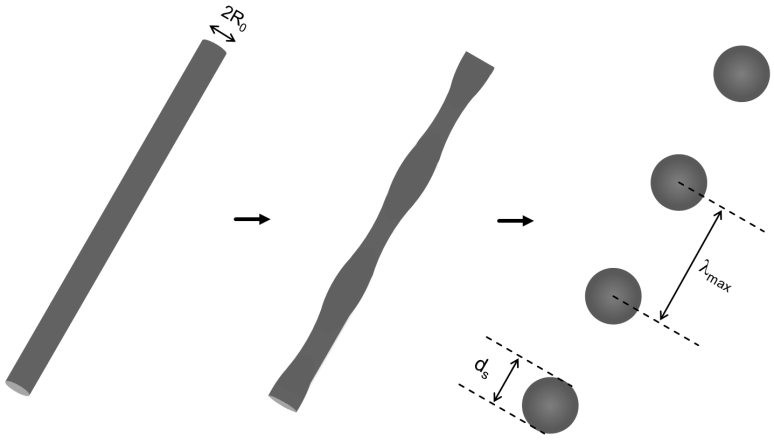

Figure 2.12: Scheme of a cylindrical nanowire transforming into a chain of nanospheres.

Although the analysis by Nichols and Mullins represents only a simplistic point of view, it can be used to describe experimental results on morphological changes of metal nanowires occuring at elevated temperatures surprisingly well. The fragmentation of Cu nanowires induced by Rayleigh instability was analyzed by Toimil-Molares et al.[77] They found results that were in excellent agreement with theoretical values. However, Karim et al. observed for polycrystalline Au nanowires significantly higher values than the calculated ones for both the distance between spheres and the sphere diameter.[79] The wires seem to be more stable than theoretically expected, which can be attributed to various effects including the stabilizing influence of the substrate. In addition, Karim et al. also demonstrated that single-crystalline Au wires, whose surface energy is not isotropic, are even more stable against fragmentation than their polycrystalline counterparts.[81]

2.4.3 Electrical transport properties

As the critical dimensions become smaller and smaller in nanowires, electrical transport properties are of interest because unusual transport phenomena can arise from one-dimensional structures.[13] The transport characteristics are influenced by composition, crystal structure, morphology, and diameter.

In one-dimensional systems two transport processes can be important: diffusive and ballistic transport. Because the length of the nanowires (regarded within this thesis) is much longer than the electron mean free path, the electrons are subjected to different scattering processes and the transport is in the diffusive regime. Ballistic transport does only occur in very thin and short nanowires and is not relevant for nanowires of practical interest.[13]

These different scattering processes have been analyzed in previous reports. In the following, size effects on carrier scattering, which can be divided in surface and grain boundary scattering, are summarized.

Surface scattering

First theoretical considerations can be traced back to studies performed by Fuchs, who investigated the influence of surface scattering of electrons on the electrical conductivity of thin metal films.[82] The work of Fuchs was extended by Sondheimer leading to the Fuchs-Sondheimer model.[83] In this well-known size effect theory, Boltzmann's transport equation is solved for the electron distribution with boundary conditions representing a thin metal film. It is assumed that the film structure is homogeneous and independent of the film thickness. Furthermore, the model is based on the free electron model.[84]

Surface scattering leads to an increase in resistivity, which is a function of the ratio k of film thickness d_f and electron mean free path l_e. The surface scattering processes are described by a single parameter

p. The specularity parameter p gives the fraction of specularly and diffusely scattered electrons. Detailed analysis can be found elsewhere.[83–85]

More complicated models for electron surface scattering in thin films and wires have been developed. For example, the theory developed by Soffer takes into account the surface roughness and the angle of incidence of scattered electrons.[86]

Scattering at grain boundaries

In thin polycrystalline metal films and wires, the grain size is comparable to the electron mean free path l_e. As a consequence, the effect of grain boundaries on the resistivity due to scattering may be significant. Mayadas and Shatzkes developed a theory that considers grain boundary scattering.[87] Changes of the electrical conductivity in the presence of grain boundaries σ_g with respect to the bulk value σ_0 are given by equation 2.17. The appropriate resistivities are denoted as ρ_0 and ρ_g, respectively.

$$\frac{\sigma_g}{\sigma_0} \equiv \frac{\rho_0}{\rho_g} = 3\left(\frac{1}{3} - \frac{1}{2}\alpha + \alpha^2 - \alpha^3 \ln\left(1 + \frac{1}{\alpha}\right)\right) \tag{2.17}$$

with

$$\alpha = \frac{R_g l_e}{1 - R_g D_g} \tag{2.18}$$

where α is a function of the mean grain size D_g, l_e, and the grain boundary reflection coefficient R_g. α increases with decreasing D_g and increasing reflectivity. In practice, the grain size is usually decreased with the film or wire thickness resulting in a higher resistivity.

3 Organization of nanowires into three-dimensional building block assemblies

3.1 Complex assemblies of nanostructures

Nanosience has reached the stage of development where different synthetic approaches can prepare not only individual nanowires but also systems of much greater complexity. In comparison to simpler 1-D nanowire systems, complex arrangements promise to exhibit improved properties and new functionalities. To fully take advantage of these peculiar properties, nanowires have to be organized into superstructures within the context of architectural design.

Presently, a variety of complex nanowire architectures has been created. The nanowire building blocks can be interconnected to complex systems in different ways as illustrated in Figure 3.1. In principle, 1-D, 2-D, and 3-D assemblies can be fabricated. The complexity and achievable integration levels are highly dependent on the interconnectivity.

Organization of nanowires into 2-D assemblies is critical to the realization of integrated electronic and photonic applications.[16] In particular, the Lieber group has developed efficient methods to align nanowires on large areas resulting in parallel and crossed nanowire structures.[88] In additon, multiple kinked (or zigzag) nanowires and rationally branched and hyperbranched 1-D nanostructures have been demonstrated.[89,90]

For applications where high integration densities are required, 3-D assemblies, such as vertically integrated arrays, networks, and hierarchical structures are more suitable (Figure 3.1). Here, research activities that center on 3-D nanowire architectures are reviewed.

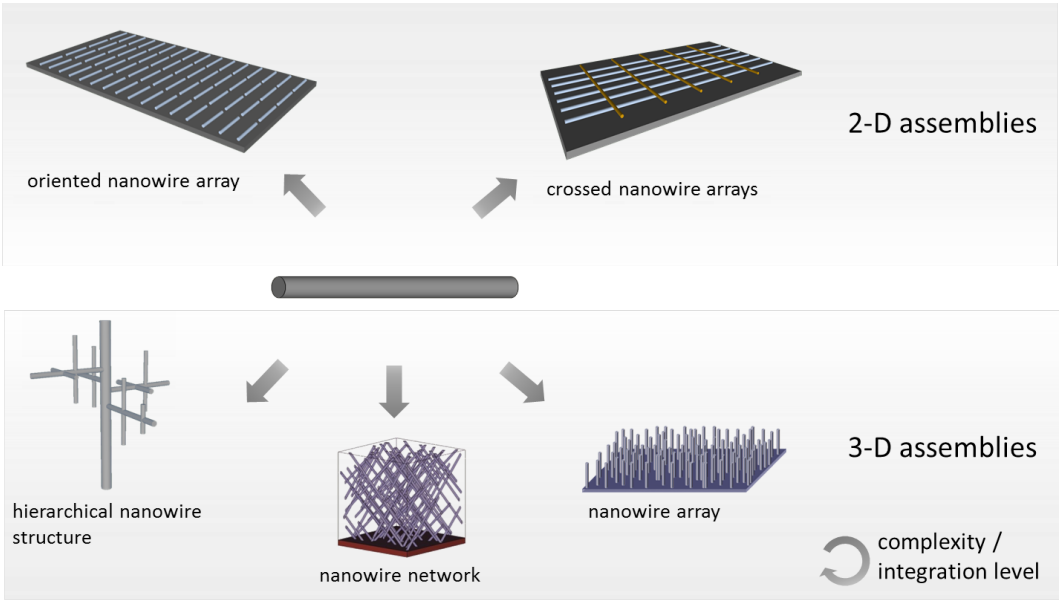

Figure 3.1: Schematic illustration of different complex nanowire structures. The depicted structures show various kinds of interconnectivity and are of different complexity.

The objectives of this chapter are the following: (i) to adress the importance of complex nanowire structures and architectural design; (ii) to provide a brief account on synthesis strategies that have been reported for 3-D nanowire assemblies; (iii) to illustrate various types of complex nanowire structures and their potential applications.

3.1.1 Why complex nanowire assemblies matter

Complex nanowire assemblies are important for several reasons. First, micro- or macroscopic nanowire superstructures provide the capability of direct device integration. The translation of the nanoscale building blocks into various device architecture can be identified as key issue, which must be addressed for realizing nanowire-based devices. This translation involves several steps as illustrated in Figure 3.2. One of the most promising approaches towards this aim are direct synthesis or assembly of nanowires into superstructures.[91]

Second, it is known that the advanced design of nanowire architectures improves properties that are important for applications. For instance, nanowire assemblies proved to be excellent electrocatalyst materials. Wang et al. demonstrated that simple palladium nanowire arrays show a higher activity for ethanol oxidation than commercially available nanoparticle catalysts.[92] The high activity is explained by effects arising from the nanowire array architecture. Furthermore, nanowire assemblies are very promising for solar conversion devices. The introduction of branches to nanowire arrays improves the light harvesting properties by several mechanisms as reported by Bierman and Jin.[93]

The integration of complex nanowire structures into devices constitutes a departure from conventional device designs. As the efficiency of nanowire structures is increased, the amounts of required material is decreased. Consequently, costs might be reduced.

Figure 3.2: Scheme illustrating the fabrication of nanowire based devices. The translation of nanowires into various device architectures involves several steps such as assembly, integration, and connection of nanoscale building blocks to electrical contacts.

3.1.2 The importance of controlled nanostructuring and architectural design

The design of a complex nanowire structure involves length scales ranging from the nanoscale building blocks to micro- or macroscopic dimensions of the nanowire superstructure. Nanostructures and their distribution in space are important for chemical and physical interactions of a functional nanowire system. Thereby, porosity is an important part of the nanowire assembly.

Whether the final process is labeled as catalysis, sensing, energy conversion, or synthesis in general, reaction rates depend on the atomic structure of active sites.[94] In addition, the local environment of these active sites is important. In porous materials, transport paths through which molecules move into or out of the material can limit the intrinsic reaction rates. Microporous channels, such as those found in zeolites, significantly hinder diffusional mass transport of molecules.[94]

Nanomaterials with high specific surface areas are desirable because these materials also can provide an extremely high density of active sites. However, accesibilty to molecules often is not assured in these

high surface area nanomaterials.[95] Sites located deep inside the material may only be reached by slow diffusion through narrow pores or are not accessible at all. Although the individual nanoparticles can show very high reaction rates, the overall activity of the nanostructured system will be much lower than if all sites were effectively exposed to molecules. Therefore, also scales above the nanoscale should be considered for nanostructure assemblies. The introduction of meso- and macrochannels facilitates mass transport processes. The porosity needs to be continuously organized, e.g., in the form of a 3-D channel network.

Current synthesis methods often do not allow to control the position and orientation of transport channels. Independent control over channel alignment and characteristics of the nanoscale components is highly desirable, since high performance requires architectural design on all length scales. In an advanced architecture, optimal structure-function relationships are present at multiple length scales.

Nature provides geometries that demonstrate extremely efficient ways how nanoscale structures can be linked to the macroscopic world. Mastering nanostructure assembly to a similar degree as nature is not possible with current methods, and it should not be regarded as ultimate goal when designing new nanowire structures. However, natural nanostructured systems can be a brilliant source of ideas.[95]

3.2 Assembly methods

Here, the intention is not to give a comprehensive overview of all synthesis methods for 3-D nanowire architectures but rather to describe the basic strategies for the fabrication of complex nanowire assemblies.

3.2.1 The bottom-up paradigm for nanotechnology

In the bottom-up approach, nanostructures are build from atomic or molecular components. Thus, morphology, structure, and composition can be controlled with atomic precision. In addition, this approach is capable of producing nanostructures in parallel.

Nanowire assemblies are available via the bottom-up paradigm for nanotechnology. Although some reports demonstrate top-down approaches for the synthesis of simple nanowire arrays, 3-D architectures can only be synthesized by bottom-up approaches, as their complexity is increased.[96,97] The challenge for nanotechnology is to organize nanowire building blocks on multiple length scales, allowing in the future to assemble any kind of hierarchical nanowire structure.

In principle, 3-D nanowire architectures can be produced via assembly of previously prepared nanowires or via direct growth approaches.

3.2.2 Assembly of nanowires

To date, 2-D nanowires assemblies have been developed by using fluidic-directed alignment, Langmuir-Blodgett techniques, electric and magnetic field alignment, surface patterns, and self-assembly.[88,98–104] Since these methods often rely on weak interactions, they are only suitable for 2-D arrangements.

A few works also reported the synthesis of 3-D nanowire structures by assembling nanowires (Figure 3.3). For example, Ou et al. demonstrated multisegmented 1-D nanostructures to form spheres in solution by self-assembly.[105] The generation of 3-D nanowire networks using diffusion bonding was reported by Gu et al.[106]

3.2.3 Direct synthesis of complex 3-D nanowire structures

Very high integration levels, which are required for many applications including energy harvesting, (electro-)catalysis, and optoelectronics, can only be achieved by 3-D assemblies.[92,97,107,108]

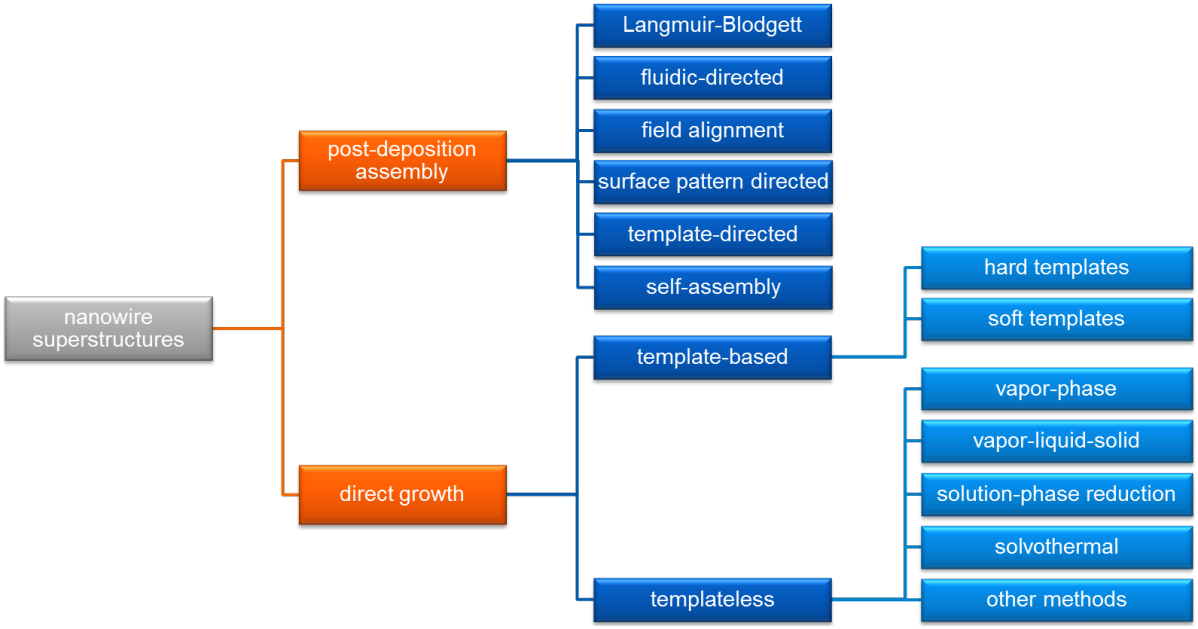

Figure 3.3: Schematic overview of general synthesis strategies for 2-D and 3-D nanowire building block assemblies.

Consequently, research in patterning of 1-D nanostructures into various device architectures has led to the synthesis of 3-D nanowire superstructures such as arrays, networks, and hierarchical structures.[24,109,110] Direct synthetic approaches are more suitable for the fabrication of these 3-D architectures. Among these direct growth methods, template-based and templateless methods are known (Figure 3.3).

Current hard template materials, including porous membranes, mesoporous silica materials, and bioorganic materials, allow precise control over the dimensions of the nanoscale building-blocks.[14,111–113] As soft templates for the direct growth of complex nanowire structures from solutions micellar networks and self-assembled surfactant systems have been reported.[114–117]

Templateless synthesis is frequently based on growth from the vapor phase, including direct and indirect vapor-phase methods.[118–121] The vapor-liquid-solid (VLS) process is also vapor-based and was employed to generate nanowire structures with a high degree of crystallinity by many research groups.[89,122–126] Thereby, 1-D growth is achieved by introducing a solid-liquid interface.

Several solution-phase reduction methods, which can be readily scaled up, have been demonstrated.[107,127–129] Moreover, synthetic approaches such as solvothermal growth and other methods (e.g., molecular beam epitaxy (MBE)) allow the synthesis of nanowire superstructures.[130,131]

3.3 3-D nanowire structures and applications

Various nanowire superstructures have been synthesized and their properties were analyzed with respect to potential applications. In this section, the intention is to demonstrate design features that are responsible for improved properties of different 3-D nanowire architectures.

3.3.1 Nanowire arrays

The production of parallel aligned nanowire arrays is a common approach to generate nanowire superstructures. Different template materials are commercially available to produce these ordered structures.

In addition, arrays can be obtained by vapor-phase methods. Due to the parallel aligned nanowires, arrays readily provide interfaces for electrical contacts.

Freestanding structures represent excellent electrode materials. If all nanowires are connected to a metal layer, good electrical conductivity will be assured. In the case of a catalycally active metal, nanowire arrays proved to show a very high catalytic activity as electrocatalyst.[92] The high activity is a direct consequence of the spatial distribution of the catalyst. Micrometer sized pores and channels in the nanowire array enable efficient mass transport. Consequently, educts easily diffuse into and products diffuse out of the nanowire structure, increasing the utilization efficiency in comparison to traditional catalyst materials.[92]

Based on the architecture, nanowire arrays made of semiconductors showed high adsorption of light and efficient collection of carriers when used as solar cell modules.[132] In a 3-D nanowire cell structure the photocarrier separation and collection can be significantly higher than in conventional thin-film cell designs.[133]

Furthermore, nanowire arrays were successfully designed to serve as a nanogenerator producing sufficient power to operate real devices.[107,134]

3.3.2 Nanowire networks

Nanowire networks are of special interest, since each individual nanowire can be directly associated in different ways with a varying number of wires, providing a large diversity of potential kinds of interconnectivity.

The term "nanowire network" is not a formalized subject and it has been used to describe various nanostructure assemblies. Here, the term is limited to structures that consist of 1-D components, which clearly can be identified as nanowires and are interconnected. Nanostructured materials such as porous metals (obtained, e.g., by dealloying) and collections of loosely bound nanowires are thus not considered as nanowire networks.[135]

General synthesis strategies for nanowire networks are based on various approches. Most notably the use of hard template materials proved to be an efficient approach to control morphology and dimensions of the building blocks precisely, whereas templateless methods, such as epitaxial growth or vapor-liquid-solid processes, demonstrated the capability to produce highly ordered nanowire superstructures.[91,112,120,121] Although some of the methods reported so far highlight the possibility to adjust more than one structural parameter, it is, however, often not possible to independently and simultaneously control several of the parameters, defining both (i) characteristics of individual nanowires, such as diameter, length, and composition, and (ii) the arrangement of nanowires into networks, determined by nanowire orientation and integration level.

With existing methods, nanowire networks were demonstrated to be promising candidates for different applications. NWNs are highly active electrocatalyst materials for several reasons, including the properties mentioned above for nanowire arrays, which are large surface areas and efficient exposure of active sites.[128] NWNs were also used as conductive support material for catalyst nanoparticles.[136] Moreover, NWNs were integrated as an active element in an ultrasensitive and highly selective gas sensor.[137] The sensitivity of nanowire-based sensors is determined by the surface-to-volume ratio of the nanowires. NWNs exhibit good structural properties for high sensitivity.

In comparison to nanowire arrays, for network structures only few applications have been reported. To overcome the limitations of current synthesis methods and apply nanowires in real-world devices, it is essential to develop new effective strategies that enable the controlled synthesis of NWNs with adjustable complexity.

3.3.3 Hierarchical nanowire structures

Highly oriented hierarchical nanowire structures are viable from vapor-phase synthetic approaches. Hyperbranched and chiral branched nanowires have been synthesized.[110,125,126] These hierarchical structures have been shown to exhibit interesting properties for applications in the field of energy harvesting.[93]

In the case of light harvesting, branched nanowire structures show improved efficiency in comparison to planar solar energy devices.[93] As origin of the improved properties following factors are suggested to be responsible. Numerous branches increase light harvesting by scattering and by increasing the quantity of absorbing structures. Consequently, the photocarrier generation is enhanced. In addition, nanowires have a short radial distance to collect the carriers.

Hierarchical nanostructures are expected to be central for the development of new functional materials because they allow optimal designs on multiple length scales. To fully use the advantages of these structures for applications, new integration methods need to be investigated.